

Top-Down Compression: Revisit Efficient Vision Token Projection for Visual Instruction Tuning

Bonan Li*
UCAS & NUS
libonan@ucas.ac.cn

Zicheng Zhang*
UCAS
zhangzicheng19@mails.ucas.ac.cn

Songhua Liu
NUS
songhua.liu@u.nus.edu

Weihao Yu
NUS
weihaoyu@u.nus.edu

Xinchao Wang[†]
NUS
xinchao@nus.edu.sg

Abstract

Visual instruction tuning aims to enable large language models to comprehend the visual world, with a pivotal challenge lying in establishing an effective vision-to-language projection. However, existing methods often grapple with the intractable trade-off between accuracy and efficiency. In this paper, we present **LLaVA-Meteor**, a novel approach designed to break this deadlock, equipped with a novel Top-Down Compression paradigm that strategically compresses visual tokens without compromising core information. Specifically, we construct a trainable *Flash Global Fusion* module based on efficient selective state space operators, which aligns the feature space while enabling each token to perceive holistic visual context and instruction preference at low cost. Furthermore, a local-to-single scanning manner is employed to effectively capture local dependencies, thereby enhancing the model’s capability in vision modeling. To alleviate computational overhead, we explore a *Visual-Native Selection* mechanism that independently assesses token significance by both the visual and native experts, followed by aggregation to retain the most critical subset. Extensive experiments show that our approach reduces visual tokens by 75%–95% while achieving comparable or superior performance across 12 benchmarks, significantly improving efficiency.

1 Introduction

Visual instruction tuning [42, 40, 31, 30] has emerged as a promising pipeline to extend large language models (LLMs) into the visual domain, achieving notable progress and demonstrating impressive performance across a wide range of vision-language tasks [27, 63, 24, 2, 47, 21], *e.g.*, image captioning [46, 62, 69], visual question answering [23, 61] and open-vocabulary object detection [22, 60]. To perceive the visual world, current mainstream approaches (*e.g.*, LLaVA [42]) typically project sequential visual tokens into the linguistic space, which are subsequently incorporated with textual representation and jointly interpreted by the LLMs decoder. However, the sheer number of visual tokens significantly increases the computational burden on LLMs. For instance, the widely used CLIP ViT-L/336px [53] encodes a single 672×1008 image into $48 \times 72 = 3456$ tokens.

To mitigate this, a variety of token compression techniques [25, 20, 57, 65, 66, 73, 9, 54] have been proposed to condense visual information into a reduced set of tokens, thereby enhancing model efficiency. Broadly, these approaches fall into two categories: Fusion and Selection. Fusion-based

*Equal Contribution

[†]Corresponding Author

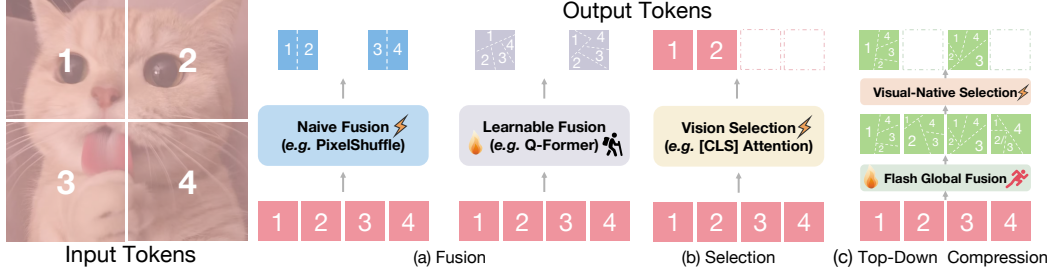


Figure 1: Illustration of visual token compression strategies. (a) Naive and learnable fusion methods reduce token count via predefined rules or learned aggregation, but may lose structural fidelity or require heavy training. (b) Vision-based selection filters important tokens using attention, yet ignores instruction relevance. (c) Our Top-Down Compression combines Flash Global Fusion for global context propagation and instruction preference summarization, with Visual-Native Selection to jointly evaluate token importance from visual and native perspectives.

methods either apply predefined merging operations (*e.g.*, PixelShuffle [28, 7, 11]), which often compromise the structural integrity of the features, or learn to condense the full token sequence into a smaller fixed set via trainable modules (*e.g.*, Q-Former [3, 30, 4, 10]), which typically require substantial additional parameters and large-scale datasets for effective training. In contrast, Selection-based approaches identify a subset of important tokens using task-agnostic visual cues (*e.g.*, class token attention [66, 43, 70]), but often overlook instruction relevance, limiting their alignment with downstream tasks.

Despite notable progress, achieving the best of both worlds—accuracy and efficiency—remains an open challenge in visual instruction tuning. Existing fusion-based compression methods typically reduce the number of tokens either by predefined merging rules or through learned token aggregation. While effective in shortening the input length, such approaches often disrupt the structural integrity of visual features or introduce significant training complexity. To address this, we introduce a novel fusion module that retains the full token sequence and enhances each token’s representation through global information propagation at low cost. Additionally, we design a dedicated instruction token that implicitly encodes instruction-level preferences by attending to the full visual context during global fusion. The instruction token is not conditioned on explicit prompts; rather, it learns to focus on instruction-relevant regions via weak supervision over large-scale vision-language data, where common user attention patterns such as phone number, faces, or salient objects are consistently reinforced. On the other hand, selection-based methods aim to identify the most important tokens using task-agnostic cues, such as attention scores from the class token. However, these approaches often overlook instruction relevance, leading to suboptimal token retention for instruction-following tasks. To mitigate this issue, we propose a native expert based on the instruction token, which complements the visual expert (class token) by providing instruction task guidance for token importance scoring. Integrating these two complementary components, we propose a unified visual token compression framework, termed Top-Down Compression. This paradigm first performs top-level global fusion to establish semantic context and task-aware priors, and subsequently applies bottom-level token selection guided by both visual and instruction-informed experts. As illustrated in Figure 1, the fusion stage (Top) facilitates holistic context exchange and distills instruction priors into the instruction token. In the subsequent selection stage (Down), each token is evaluated from two perspectives: a visual expert that highlights globally salient regions, and a native expert that captures task-specific relevance. Based on these complementary signals, we select a compact and informative token subset to be forwarded to the LLMs, thereby achieving an effective balance between semantic richness and computational efficiency.

Building upon the proposed Top-Down Compression strategy, we present a novel and efficient vision-language model named **LLaVA-Meteor**, which comprises two key components: Flash Global Fusion (FGF) and Visual-Native Selection (VNS). In the FGF module, we leverage state space models (SSMs) [15] as the core operator due to their linear computational complexity and strong capability for long-range sequence modeling. This enables efficient propagation of global contextual information across the visual token sequence. To further enhance spatial understanding, we incorporate a local-to-single scanning strategy, which captures local dependencies by summarizing information from spatial

neighborhoods before each token. In addition, a learnable instruction token is inserted at the center of the token sequence and trained to aggregate holistic semantic information while implicitly encoding instruction-related cues. In the VNS module, we adopt a dual-expert evaluation mechanism. The class token, obtained from a frozen vision encoder, serves as a visual expert and provides attention-based scores to reflect general visual importance. Meanwhile, the instruction token, enriched by the Flash Global Fusion module, serves as a native expert that evaluates instruction relevance by computing its similarity with each token in the sequence. To synthesize these two complementary perspectives, we aggregate their scores at each token index and select the Top- K tokens with the highest combined importance as the final visual input to the LLMs.

In summary, our contributions can be summarized as follows: (i) We construct the vision-language model LLaVA-Meteor upon the simple and effective Top-Down Compression paradigm, simultaneously achieving strong performance and high efficiency; (ii) We introduce a lightweight fusion module, Flash Global Fusion, which enables rapid global interaction and accurately distills instruction preferences; (iii) We propose an innovative hybrid selection strategy, Visual-Native Selection, which jointly assesses token importance through a visual and a native expert to guide the selection process; (iv) Extensive evaluations demonstrate competitive or superior performance across a wide range of benchmarks while significantly reducing the number of visual tokens.

2 Related Work

Visual instruction tuning has become a cornerstone in extending large language models to understand and reason over visual content under textual instructions [18, 64, 39, 45, 37, 58, 64]. Early works such as Flamingo [1] and BLIP-2 [30] explored aligning vision-language representations through contrastive learning or image-caption matching objectives, demonstrating effectiveness in image-text retrieval and captioning. However, these models lacked flexible instruction-following capabilities. To bridge this gap, recent methods have introduced explicit multimodal instruction tuning. LLaVA [42] established a lightweight yet effective pipeline by projecting CLIP-encoded image features into an LLMs (e.g., Vicuna) via a learnable MLP. This approach enabled strong instruction-following performance across multiple vision-language tasks and inspired variants like LLaVA-1.5 [40], which incorporated high-resolution image handling and OCR-specific improvements. MiniGPT-4 [72], InstructBLIP [52], Qwen-VL [3], and CogVLM [62] further advanced this line by introducing multi-stage pretraining, hierarchical perception, or better instruction synthesis. Despite their success, these models are constrained by the large number of visual tokens injected into the LLMs, which significantly increases memory and latency. This has motivated a growing body of research on efficient visual token projection.

Efficient vision token projection aims to reduce the number of visual tokens passed into the language model while maintaining sufficient semantic fidelity for instruction understanding [12, 34, 5, 54, 32]. Existing approaches in this space predominantly compress visual inputs through feature fusion, token selection, or hybrid strategies. Q-Former [30] and Resampler [3] use trainable queries to aggregate visual context into fixed-length representations, which can then be fused with textual inputs. These architectures significantly reduce token count but may lose fine-grained visual cues, especially in high-resolution settings. FocusLLaVA [73] addresses this by introducing dual expert samplers guided by both visual and textual attention, effectively improving relevance alignment under compression. TokenPacker [33] injects high-resolution visual details into a compressed representation through a dynamic slicing and reassembly scheme. Meanwhile, LLaVA-Mini [71] explores extreme compression, reducing image input to a single token using query-based fusion and modality pre-fusion, albeit with potential semantic loss in complex scenes. Other methods such as VisionZip [66], LDPv2 [10], and Abstractor [4] explore various forms of spatial pooling or local detail preservation, but often focus on either visual saliency or computational efficiency alone, without considering instruction priors. In contrast to prior efforts, our work introduces a Top-Down Compression framework that explicitly incorporates instruction-aware global fusion before performing token filtering.

3 Methodology

In this section, we first present the overall framework of LLaVA-Meteor, which generates instruction-following responses conditioned on visual inputs (Section 3.1). We then detail its two key components

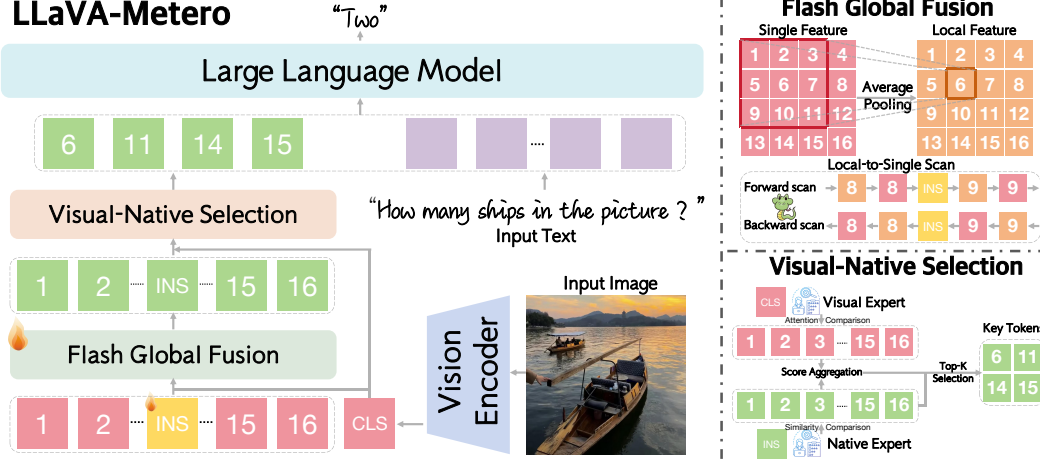


Figure 2: Overview of the proposed LLaVA-Meteor, which adopts a two-stage Top-Down Compression pipeline to efficiently project visual tokens for instruction-following tasks. An input image is first encoded by a vision encoder into dense visual tokens, including a class token (CLS). We omitted the partitioning step for a clearer presentation. The Flash Global Fusion module (Top) propagates semantic context and instruction-level priors through efficient global interactions, enhanced by a local-to-single scanning strategy that improves local awareness. A learnable instruction token (INS) is inserted to aggregate task-relevant cues during fusion. Subsequently, the Visual-Native Selection module (Down) evaluates token importance from two perspectives: a class-based visual expert and an instruction-based native expert. Their scores are aggregated to select a compact set of key tokens, which are passed to the large language model along with the input to generate the final response.

for efficient visual token compression: Flash Global Fusion (Section 3.2) and Visual-Native Selection (Section 3.3). Following the proposed Top-Down Compression, our method enables high-resolution image understanding while significantly reducing memory and computational overhead.

3.1 Overview of LLaVA-Meteor

We build our model upon the widely used high-resolution vision-language framework LLaVA-UHD [16], and the overall architecture is illustrated in Figure 2. Given an input image $I \in \mathbb{R}^{H \times W \times 3}$ with arbitrary resolution and aspect ratio, we follow the LLaVA-UHD strategy by first partitioning the image into N variable-sized sub-images $\{I_j\}_{j=0}^N$, where I_0 denotes the resized global image. This partitioning facilitates scalable and efficient encoding of high-resolution content. Each sub-image I_j is processed by a pre-trained vision encoder, CLIP ViT-L/336px [53], which produces a sequence of visual tokens $\{T_j\} \in \mathbb{R}^{(H_u W_u) \times C}$ along with a corresponding class token $CLS_j \in \mathbb{R}^{1 \times C}$. To simultaneously achieve high accuracy and efficiency, we replace the original token compression layer with our proposed Flash Global Fusion and Visual-Native Selection modules. Through the Top-Down Compression, only the Top- K most informative tokens $\{F_j\} \in \mathbb{R}^{K \times D}$, where $K \ll H_t \times W_t$, are retained from each sub-image. Finally, the compressed token sequences $\{F_j\}_{j=0}^N$ are concatenated and combined with the instruction text. This multimodal input is then fed into a large language model, such as Vicuna [8], to generate the corresponding instruction-following response.

3.2 Flash Global Fusion

To enrich the representational capacity of visual tokens before compression, we introduce a global context modeling module that enables efficient long-range interaction and instruction-aware feature enhancement. Unlike prior fusion strategies that directly reduce token count at the cost of information loss, our approach retains the full token sequence while refining its contextual semantics, thereby laying a strong foundation for the subsequent selection stage.

Global Context Propagation. To this end, we employ state space models (SSMs) as the core computational operator due to their ability to model long sequences with linear complexity. In

particular, we adopt the advanced selective scan SSMs introduced by Mamba [14] as a lightweight yet effective backbone, enabling fast and global context propagation across the token sequence. This allows each token to incorporate holistic information from other tokens within the same sub-image, while maintaining high throughput on long visual sequences. To compensate for the lack of 2D spatial inductive bias in Mamba, we propose a local-to-single scanning strategy that explicitly enhances local spatial modeling. Specifically, before processing i^{th} token T^i (Omit the index of sub-image for clarity), we first gather its local context by constructing a 3×3 window centered around the target token in the 2D feature map. This window captures the immediate spatial neighborhood, which is critical for modeling visual patterns. Then, we perform spatial downsampling on these tokens within the window, aggregating them into a single representative token as TL^i . Therefore, our local-to-single scanning strategy can be succinctly expressed as follows:

$$\begin{aligned} \text{forward scan} : TL^{i-1} &\rightarrow T^{i-1} \rightarrow TL^i \rightarrow T^i \rightarrow TL^{i+1} \rightarrow T^{i+1}, \\ \text{backward scan} : T^{i-1} &\leftarrow TL^{i-1} \leftarrow T^i \leftarrow TL^i \leftarrow T^{i+1} \leftarrow TL^{i+1}. \end{aligned} \quad (1)$$

Here, we reverse the scan order within the arrangement of token sequence to capture robust features. This allows us to perform the global context propagation follows:

$$\{F^i\}_{i=1}^{H_u W_u} = SSMs(L2Sscan(\{TL^i\}_{i=1}^{H_u W_u}, \{T^i\}_{i=1}^{H_u W_u})), \quad (2)$$

where $L2Sscan(\cdot)$ denotes the local-to-single and $\{F^i\}_{i=1}^{H_u W_u}$ denotes the outputs tokens.

Instruction Preference Summarization. Additionally, we insert a shared learnable instruction token, denoted as $INS \in \mathbb{R}^{1 \times C}$, into the center of each sub-image’s token sequence prior to the fusion process. This instruction token is trained to implicitly capture instruction-relevant cues by attending to the full visual context during global context propagation. As a result, it serves as a task-aware prior that guides the token selection process in subsequent Visual-Native Selection stage.

3.3 Visual-Native Selection

Following the enriched token representations produced by the Flash Global Fusion module, we apply a Visual-Native Selection mechanism to perform token compression. This module evaluates the importance of each token from two complementary perspectives: visual significance and instruction relevance, aiming to select the most informative subset for downstream language modeling. By leveraging both a general visual expert and a task-aware native expert, this dual-expert strategy allows the model to retain semantically critical tokens while eliminating redundant ones, thereby significantly improving computational efficiency without compromising task performance.

Visual Expert Scoring. To capture general visual importance, we utilize the class token from the frozen vision encoder as a visual expert, as it is known to encode global semantic information. Specifically, we measure the importance of each visual token by computing its attention weight with respect to the class token, serving as a proxy for visual saliency:

$$VS_j^i = \frac{AttnScore(CLS, T^i)}{\sum_{i=1}^{H_u W_u} AttnScore(CLS, T^i)}, \quad (3)$$

where VS^i denotes the visual importance score for the i^{th} token, and $AttnScore(\cdot)$ is derived from the attention map of the frozen vision encoder. Note that the attention distribution includes the self-attention of the class token itself, which causes the total attention over the other tokens to deviate from 1. To address this, we normalize the attention weights across all non-class tokens to form a valid probability distribution. This ensures that the visual expert scores are both interpretable and comparable across different sub-images. By this design, tokens receiving higher scores from the class token are regarded as more visually informative, as they typically correspond to salient objects, prominent regions, or semantically meaningful structures within the image.

Native Expert Scoring. Complementing the general-purpose visual expert, the native expert is designed to capture instruction preferences. We leverage the instruction token, which is optimized within the Flash Global Fusion module, as a task-aware representation trained to encode high-level

semantic intent under vision-language supervision. To evaluate instruction relevance, we compute the similarity between each token and the instruction token using a softmax-normalized dot product:

$$NS^i = \frac{e^{\langle F^i, INS \rangle}}{\sum_{i=1}^{H_u W_u} e^{\langle F^i, INS \rangle}}, \quad (4)$$

where NS^i denotes the instruction-aware score of the i^{th} token, and F^i is the token output from the Flash Global Fusion module. To ensure compatibility with the visual expert scores in terms of numerical scale, we apply the softmax operation over all tokens in the same sub-image. This transforms both expert scores into probability-like weights, enabling stable and interpretable fusion in the subsequent selection stage. By leveraging the instruction alignment encoded in instruction token, the model is able to identify semantically important tokens even when they correspond to visually subtle features, thereby overcoming the limitations of saliency-based compression methods.

Score Aggregation and Top- K Selection. To integrate the complementary signals from both experts, we compute a fused importance score for each token via weighted aggregation:

$$AS^i = \lambda \cdot VS^i + (1 - \lambda) \cdot NS^i, \quad (5)$$

where $\lambda \in [0, 1]$ controls the relative contributions of the visual and native experts. Here, we set $\lambda = 0.8$ as the default value, as it consistently yields favorable performance across multiple datasets. Nevertheless, dataset-specific tuning of λ may further improve performance in certain cases. To facilitate stable convergence during early training, we adopt a progressive weighting scheme: the native expert’s contribution is linearly increased from 0 to $1 - \lambda$ over the first few training epochs. Once the aggregated scores $\{AS_j^i\}$ are obtained, we perform token selection over the output sequence from the Flash Global Fusion module, rather than the raw visual tokens. Specifically, we select the Top- K tokens with the highest fused scores:

$$\mathcal{Q}_K = \text{Top}K \left(\{AS_j^i\}_{i=1}^{H_u W_u} \right), \quad \{F^i\}_{i \in \mathcal{Q}_K} \subseteq \{F^i\}_{i=1}^{H_u W_u}, \quad (6)$$

where \mathcal{Q}_K denotes the indices of the selected tokens. This ensures that the retained subset is derived from the enriched sequence, which integrates both global visual context and instruction relevance, thereby maximizing informativeness while maintaining a compact input for the LLMs.

4 Experiments

In this section, we present a comprehensive empirical evaluation of LLaVA-Meteor to assess its performance. We begin by detailing the implementation setup (Section 4.1 and 4.2), followed by an analysis of results across nine widely-used benchmarks in comparison with state-of-the-art models (Section 4.3). Finally, we provide further insights through interpretive analyses (Section 4.4).

4.1 Implementation Details

Our model, LLaVA-Meteor, is constructed based on the widely-used frameworks of LLaVA-1.5 [40] and LLaVA-UHD [16]. Specifically, we employ pre-trained CLIP ViT-L/336px [53] as the visual encoder, operating at a default resolution of 336×336 to obtain $24 \times 24 = 576$ tokens. Language component is powered by Vicuna-13B [8], and we replace the standard compression layer with our proposed Top-Down Compression module, serving as the projection module linking vision and language. During image slicing, minor adjustments (up to 7–8 pixels) may be made to ensure compatibility with patch-based processing. We follow LLaVA-UHD to slice each input image into N sub-images, the total number of visual tokens passed to the language model becomes $32 \times (N + 1)$, including those from a low-resolution global view. We cap N at 6, enabling support for images up to 672×1008 in resolution. In pretraining phase, only the Top-Down Compression module is trained for one full epoch. We apply the AdamW optimizer with a learning rate of 1×10^{-3} and a cosine decay schedule. The global batch size is set to 256. This phase takes approximately 3 hours on 8 H800 GPUs. For instruction tuning, the visual encoder is kept fixed while both the visual compression and



Figure 3: Qualitative comparison of LLaVA-UHD and our LLaVA-Meteor.



Figure 4: Qualitative comparisons for different expert selection strategies.

the language model are fine-tuned. The learning rate is reduced to 2×10^{-5} , and the batch size is set to 128. Other training configurations remain consistent with the first stage. This stage requires approximately 10 hours on the same hardware.

4.2 Datasets and Benchmarks

Datasets. We follow the training datasets as LLaVA-UHD [16]. In the first stage, we utilize CC-595K dataset [40] to finetune the projector. In the second stage, for normal resolution model, we use the dataset consists of a diverse mixture of 656K samples, drawn from LLaVA-Instruct [42], TextCaps [55], GQA [19], OCR-VQA [51], and Visual Genome [26] for instruction tuning.

Benchmarks. We adopt 12 popular benchmarks to evaluate our model, including: (1) text-oriented VQA such as TextVQA (VQA^T) [56], DocVQA (VQA^D) [50], ChartQA (QA^C) [48] and InfoVQA (VQA^I) [49]; (2) general VQA such as GQA [19], VQA^{v2} [13] and VizWiz [17]; (3) comprehensive evaluation such as MMB [44], MMVet [67], MMMU [68], POPE [36] and SEED [29].

4.3 Compared with SOTA Methods

We conduct a comprehensive comparison between our proposed LLaVA-Meteor and prior state-of-the-art vision-language models, with a particular focus on LLaVA-UHD, upon which our work is built. The results in Table 1 demonstrate that our model achieves competitive or superior performance across diverse benchmarks while utilizing significantly fewer visual tokens. Since images may

Table 1: Comparison of recent vision-language models across text-oriented VQA, general VQA, and comprehensive benchmarks.

Model	LLM	PT/IT	Token	VQA ^T	VQA ^D	QA ^C	VQA ^I	GQA	VQA ^{v2}	VizWiz	MMB	MMVet	MMMU	POPE	SEED	Avg
MobileVLM V2 [10]	MobileLlama-2-7B	1.2M/3.6M	144	52.1	-	-	-	59.3	-	-	-	-	-	84.3	-	-
BLIP-2 [30]	Vicuna-13B	129M/-	32	42.5	-	-	-	41.0	65.0	19.6	-	-	-	85.3	49.7	-
Insturct-BLIP [52]	Vicuna-7B	129M/1.2M	64	50.1	-	-	-	49.5	-	34.5	-	26.3	-	-	-	-
QwenVL [3]	Qwen-7B	1.4B/50M	256	63.8	65.1	65.7	-	59.3	78.8	35.2	-	-	-	-	62.3	-
VILA [38]	Llama2-7B	50M/1M	576	64.4	-	58.6	-	62.3	79.9	57.8	68.9	34.9	-	85.5	-	-
MobileVLM V2 [10]	Vicuna-7B	1.2M/3.6M	144	62.3	-	-	-	62.6	-	-	-	-	-	85.3	-	-
Mini-Gemini [35]	Vicuna-7B	1.2M/1.5M	576	65.9	-	-	-	-	-	68.5	46.0	38.1	-	-	-	-
LLaVA-1.5 [40]	Vicuna-7B	558K/665K	576	58.2	28.1	-	25.8	63.3	78.5	50.0	64.3	31.1	35.3	85.9	66.1	-
TokenPacker [33]	Vicuna-7B	558K/665K	144	-	-	-	-	61.9	77.9	52.0	65.1	33.0	-	87.0	-	-
InternVL2 [6]	Internlm2.5-7B	558K/665K	256	49.7	26.9	18.1	21.8	63.0	77.8	50.6	70.9	34.1	39.2	86.8	71.1	50.8
<i>High-resolution LLMs</i>																
Monkey [37]	Qwen-7B	-1.44M	~1024	67.7	66.5	36.1	-	60.7	80.3	61.2	-	-	-	-	-	-
TokenPacker-HD [33]	Vicuna-7B	1.2M/1.5M	~954	68.0	60.2	-	-	-	81.2	54.7	67.4	-	35.4	-	-	-
Mini-Gemini-HD [35]	Vicuna-7B	1.2M/1.5M	2880	68.4	65.0	-	-	-	80.3	54.6	65.8	41.3	36.8	86.8	-	-
FastViTHD [59]	Qwen2-7B	558K/1.1M	256	64.4	-	-	-	-	63.1	-	-	-	-	88.1	-	-
LLaVA-UHD [16]	595K/665K	-256	67.7	62.6	56.3	36.8	63.8	81.7	56.1	68.0	42.1	35.5	89.1	65.6	60.4	60.4
LLaVA-NeXT [41]	Vicuna-7B	558K/765K	~2880	64.9	74.4	54.8	37.1	64.2	81.8	57.6	68.1	43.9	35.8	86.5	68.2	61.4
InternVL2-HD [6]	Internlm2.5-7B	558K/770K	~1282	65.6	72.6	69.8	30.9	63.2	78.9	56.3	72.1	35.7	39.9	87.3	73.4	62.1
<i>Ours</i>																
LLaVA-Meteor	Vicuna-13B	595K/665K	~256	69.9	64.2	59.0	39.2	64.9	82.4	59.3	69.4	44.7	37.5	89.9	67.7	62.4
compare to LLaVA-UHD			100%	+2.2	+1.6	+2.7	+2.4	+1.1	+0.7	+3.2	+1.4	+2.6	+2.0	+0.8	+2.1	+2.0
LLaVA-Meteor	Vicuna-13B	595K/665K	~114	68.3	63.1	58.6	37.7	64.6	81.8	57.1	68.4	42.7	34.6	88.7	66.9	61.0
compare to LLaVA-UHD			44.5%	+0.6	+0.5	+2.3	+0.9	+0.8	+0.1	+1.0	+0.4	+0.6	-0.8	-0.5	+1.3	+0.6
LLaVA-Meteor	Vicuna-13B	595K/665K	~56	65.0	58.4	56.5	37.1	62.4	81.2	55.3	68.0	41.6	34.2	87.2	64.8	59.3
compare to LLaVA-UHD			21.8%	-2.7	-4.2	+0.2	+0.3	-1.4	-0.5	-0.8	+0.0	-0.5	-1.3	-1.9	-0.8	-1.1

be divided into different numbers of sub-images depending on their resolution and aspect ratio, we report the average number of visual tokens per image across datasets in the table. For clarity and fair comparison, we refer to the token count per sub-image when describing and analyzing model behavior throughout the text. Specifically, when using the same token budget as LLaVA-UHD (144 tokens for on sub-images), LLaVA-Meteor yields consistent improvements on almost all tasks, including 69.9 on VQA^T, 39.2 on VQA^I, 64.9 on GQA, 82.4 on VQA^{v2} and 89.9 on POPE. These gains indicate enhanced comprehension in both text-oriented and reasoning-heavy vision-language scenarios. Notably, the average performance increases by +2.0 points, validating the overall robustness of our approach. More impressively, when we reduce the token count to 64 and 32—representing 20% and 5% of the original token length for on sub-images—LLaVA-Meteor still maintains strong performance. For instance, with only 64 tokens, our model still achieves 58.6 on QA^C and 66.9 on SEED, with only a marginal drop of -0.4 and -0.8 compared to the 144-token setting, while significantly improving efficiency. Compared to LLaVA-UHD, even our most compressed 32-token variant retains competitive accuracy while reducing token usage by over 95%. This highlights the effectiveness of our Top-Down Compression framework, which selects a semantically rich token subset without sacrificing representational fidelity. To provide a more intuitive illustration of the effectiveness of LLaVA-Meteor, we further visualize the input image, instruction, and the corresponding response, as shown in Figure 3. Overall, our method demonstrates a compelling balance between performance and computational cost, making it highly suitable for resource-constrained scenarios and real-world deployments.

4.4 Ablation Study

Scanning Strategies. We conduct an ablation study to assess the impact of different scanning strategies within the Flash Global Fusion module. Specifically, we compare three configurations: (i) the single scan strategy, which processes tokens sequentially without local context modeling; (ii) the local-to-single scan strategy, which enhances each token representation by aggregating its 3×3 spatial neighborhood before propagation. Experimental results in Table 2 demonstrate that the local-to-single scan strategy consistently achieves better performance than the single scan strategy. This highlights the importance of integrating local spatial dependencies, especially in scenarios requiring fine-grained visual understanding. Furthermore, we also attempt to combined these two strategy but find it only provides marginal improvements over the local-to-single, the gains are not significant and come at the cost of 50% additional computation in compression modules. In light of these findings, we adopt the local-to-single scan strategy as the default configuration in all experiments, as it offers a favorable balance between accuracy and efficiency. Additionally, we recommend that when operating on high-resolution feature maps, the local window size can be further increased (e.g., to 5×5 or 7×7) to enable richer multi-scale context modeling and improve the perception of spatial hierarchies.

Table 2: Comparison of different scanning strategies.

Scan Strategy	VQA ^T	VQA ^D	QA ^C	VQA ^I	GQA	VQA ^{v2}	VizWiz	MMB	MMVet	MMMU	POPE	SEED	Avg
Single	68.9	63.0	58.1	38.4	64.0	81.8	57.5	68.1	42.0	37.5	88.7	65.4	61.1
Local-to-Single	69.9	64.2	59.0	39.2	64.9	82.4	59.3	69.4	44.7	37.5	89.9	67.7	62.4

Table 3: Comparison of different expert selection strategies.

Expert Selection Strategy	VQA ^T	VQA ^D	QA ^C	VQA ^I	GQA	VQA ^{v2}	VizWiz	MMB	MMVet	MMMU	POPE	SEED	Avg
Visual	69.7	63.5	59.3	37.8	63.8	82.1	57.2	66.9	41.7	38.1	88.0	65.5	61.1
Native	67.1	62.3	57.7	37.9	61.9	79.4	56.6	66.2	40.0	31.1	86.8	63.4	59.2
Visual-Native	69.9	64.2	59.0	37.8	64.9	82.4	59.3	69.4	44.7	37.5	89.9	67.7	62.4

Expert Selection Strategies. To better understand the roles of different expert signals in our Visual-Native Selection module, we conduct ablation studies comparing three configurations for Top- K token selection: (i) using only the visual expert, (ii) using only the native expert, and (iii) using both experts jointly via weighted aggregation. Experimental results in Table 3 show that for tasks requiring dense prediction, such as object understanding, the performance of using only the visual expert is comparable to that of the combined visual-native expert. This suggests that the visual expert, which originates from a pre-trained vision encoder, is sufficient to capture general semantic structure in these scenarios. However, in more challenging tasks that involve reasoning and attribute discrimination, the visual-native configuration demonstrates a clear advantage. The native expert contributes instruction-aware cues that enhance the model’s ability to focus on contextually important but visually less prominent tokens, leading more accurate alignment with task objectives. In contrast, relying solely on the native expert results in inferior performance. This approach requires the model to learn task-specific knowledge entirely from vision-language supervision without support from visual encoder. Such reliance not only reduces overall accuracy but also leads to unstable training behavior, especially in the early training stages, as indicated by more frequent and larger fluctuations in the loss values. To facilitate a clearer understanding of the patch selection behavior of each expert, we present detailed visualizations in Figure 4. Based on these observations, we recommend using both experts in combination. The weighting parameter λ between the two experts can be adjusted to suit the nature of the task. For example, lower values of λ are preferable in instruction-focused domains, while higher values can be beneficial when visual saliency dominates. In our default configuration, we set $\lambda = 0.8$, as it yields consistently strong results across a variety of benchmarks.

Model Efficiency. To validate the efficiency of our proposed framework, we conduct a comprehensive ablation study across four three aspects: model size (parameter count), training time, and TPS (token per second). Note that we only present the parameters of the projector here. We compare our method against sota LLaVA-UHD under identical hardware settings and input resolutions. Experimental results in Table 4 demonstrate that our model consistently achieves favorable efficiency across all metrics. In particular, the overall parameter remains competitive due to the lightweight design of the Flash Global Fusion and training-free Visual-Native Selection modules. More notably, the computational cost is significantly reduced as a result of effective token compression. Since fewer visual tokens are forwarded to the language model, both training and inference stages benefit from lower memory usage and shorter runtime. As the number of retained tokens decreases, we observe the increase in TPS, confirming that token compression directly translates to computational savings. This property makes our model highly suitable for deployment in resource-constrained scenarios or applications requiring real-time response. Overall, the proposed architecture provides a balanced solution that preserves task performance while substantially improving computational efficiency.

Table 4: Efficiency comparison with different model.

Model	Tokens	Parameters	Train	TPS	Avg
LLaVA-UHD [16]	144	137.84M	17.2h	28.4	60.4
LLaVA-Meteor	144	37.08M	13.7h	29.1	62.4
LLaVA-Meteor	64	37.08M	12.9h	31.3	61.0
LLaVA-Meteor	32	37.08M	12.1h	32.9	59.3

5 Conclusion

In this paper, we revisit the challenge of efficient vision token projection in the context of visual instruction tuning and introduce a novel compression framework termed Top-Down Compression. By explicitly integrating global fusion with expert-guided token selection, our method effectively bridges

the gap between performance and efficiency. Specifically, the proposed Flash Global Fusion module enables lightweight yet holistic context propagation, while the Visual-Native Selection strategy jointly evaluates token significance from both semantic and instruction-aware perspectives. Built upon this paradigm, our model LLaVA-Meteor achieves state-of-the-art or competitive performance across a wide range of vision-language benchmarks, with up to 75%–95% reduction in visual tokens. These results demonstrate that our approach not only preserves semantic fidelity but also significantly enhances computational efficiency, making it well-suited for real-world, resource-constrained applications. We hope this work offers a new perspective on balancing compression and task alignment for future vision-language modeling.

References

- [1] Jean-Baptiste Alayrac, Jeff Donahue, Pauline Luc, Antoine Miech, Iain Barr, Yana Hasson, Karel Lenc, Arthur Mensch, Katherine Millican, Malcolm Reynolds, et al. Flamingo: a visual language model for few-shot learning. In *NeurIPS*, pages 23716–23736, 2022.
- [2] Md Adnan Arefeen, Biplob Debnath, Md Yusuf Sarwar Uddin, and Srimat Chakradhar. Vita: An efficient video-to-text algorithm using vlm for rag-based video analysis system. In *CVPR*, pages 2266–2274, 2024.
- [3] Jinze Bai, Shuai Bai, Shusheng Yang, Shijie Wang, Sinan Tan, Peng Wang, Junyang Lin, Chang Zhou, and Jingren Zhou. Qwen-vl: A frontier large vision-language model with versatile abilities. *arXiv preprint arXiv:2308.12966*, 1(2):3, 2023.
- [4] Junbum Cha, Wooyoung Kang, Jonghwan Mun, and Byungseok Roh. Honeybee: Locality-enhanced projector for multimodal llm. In *CVPR*, pages 13817–13827, 2024.
- [5] Liang Chen, Haozhe Zhao, Tianyu Liu, Shuai Bai, Junyang Lin, Chang Zhou, and Baobao Chang. An image is worth 1/2 tokens after layer 2: Plug-and-play inference acceleration for large vision-language models. In *ECCV*, pages 19–35, 2024.
- [6] Zhe Chen, Weiyun Wang, Hao Tian, Shenglong Ye, Zhangwei Gao, Erfei Cui, Wenwen Tong, Kongzhi Hu, Jiapeng Luo, Zheng Ma, et al. How far are we to gpt-4v? closing the gap to commercial multimodal models with open-source suites. *Science China Information Sciences*, 67(12):220101, 2024.
- [7] Zhe Chen, Jiannan Wu, Wenhai Wang, Weijie Su, Guo Chen, Sen Xing, Muyan Zhong, Qinglong Zhang, Xizhou Zhu, Lewei Lu, et al. Internvl: Scaling up vision foundation models and aligning for generic visual-linguistic tasks. In *CVPR*, pages 24185–24198, 2024.
- [8] Wei-Lin Chiang, Zhuohan Li, Ziqing Lin, Ying Sheng, Zhanghao Wu, Hao Zhang, Lianmin Zheng, Siyuan Zhuang, Yonghao Zhuang, Joseph E Gonzalez, et al. Vicuna: An open-source chatbot impressing gpt-4 with 90%* chatgpt quality. See <https://vicuna.lmsys.org> (accessed 14 April 2023), 2(3):6, 2023.
- [9] Rohan Choudhury, Guanglei Zhu, Sihan Liu, Koichiro Niinuma, Kris Kitani, and László Jeni. Don’t look twice: Faster video transformers with run-length tokenization. In *NeurIPS*, pages 28127–28149, 2024.
- [10] Xiangxiang Chu, Limeng Qiao, Xinyu Zhang, Shuang Xu, Fei Wei, Yang Yang, Xiaofei Sun, Yiming Hu, Xinyang Lin, Bo Zhang, et al. Mobilevlm v2: Faster and stronger baseline for vision language model. *arXiv preprint arXiv:2402.03766*, 2024.
- [11] Xiaoyi Dong, Pan Zhang, Yuhang Zang, Yuhang Cao, Bin Wang, Linke Ouyang, Songyang Zhang, Haodong Duan, Wenwei Zhang, Yining Li, et al. Internlm-xcomposer2-4khd: A pioneering large vision-language model handling resolutions from 336 pixels to 4k hd. In *NeurIPS*, pages 42566–42592, 2024.
- [12] Mingze Gao, Jingyu Liu, Mingda Li, Jiangtao Xie, Qingbin Liu, Bo Zhao, Xi Chen, and Hui Xiong. Tc-llava: Rethinking the transfer from image to video understanding with temporal considerations. *arXiv preprint arXiv:2409.03206*, 2024.

- [13] Yash Goyal, Tejas Khot, Douglas Summers-Stay, Dhruv Batra, and Devi Parikh. Making the v in vqa matter: Elevating the role of image understanding in visual question answering. In *CVPR*, pages 6904–6913, 2017.
- [14] Albert Gu and Tri Dao. Mamba: Linear-time sequence modeling with selective state spaces. *arXiv preprint arXiv:2312.00752*, 2023.
- [15] Albert Gu, Karan Goel, and Christopher Re. Efficiently modeling long sequences with structured state spaces. In *ICLR*, 2022.
- [16] Zonghao Guo, Ruyi Xu, Yuan Yao, Junbo Cui, Zanlin Ni, Chunjiang Ge, Tat-Seng Chua, Zhiyuan Liu, and Gao Huang. Llava-uhd: an lmm perceiving any aspect ratio and high-resolution images. In *ECCV*, pages 390–406, 2024.
- [17] Danna Gurari, Qing Li, Abigale J Stangl, Anhong Guo, Chi Lin, Kristen Grauman, Jiebo Luo, and Jeffrey P Bigham. Vizwiz grand challenge: Answering visual questions from blind people. In *CVPR*, pages 3608–3617, 2018.
- [18] Wenbo Hu, Yifan Xu, Yi Li, Weiye Li, Zeyuan Chen, and Zhuowen Tu. Bliva: A simple multimodal llm for better handling of text-rich visual questions. In *AAAI*, pages 2256–2264, 2024.
- [19] Drew A Hudson and Christopher D Manning. Gqa: A new dataset for real-world visual reasoning and compositional question answering. In *CVPR*, pages 6700–6709, 2019.
- [20] Shibo Jie, Yehui Tang, Jianyuan Guo, Zhi-Hong Deng, Kai Han, and Yunhe Wang. Token compensator: Altering inference cost of vision transformer without re-tuning. In *ECCV*, pages 76–94, 2024.
- [21] Er Jin, Qihui Feng, Yongli Mou, Gerhard Lakemeyer, Stefan Decker, Oliver Simons, and Johannes Stegmaier. Logicad: Explainable anomaly detection via vlm-based text feature extraction. In *AAAI*, pages 4129–4137, 2025.
- [22] Sheng Jin, Xueying Jiang, Jiaxing Huang, Lewei Lu, and Shijian Lu. Llms meet vlms: Boost open vocabulary object detection with fine-grained descriptors. In *ICLR*, 2024.
- [23] Mahmoud Khademi, Ziyi Yang, Felipe Frueger, and Chenguang Zhu. Mm-reasoner: A multi-modal knowledge-aware framework for knowledge-based visual question answering. In *EMNLP*, pages 6571–6581, 2023.
- [24] Junsu Kim, Yunhoe Ku, Jihyeon Kim, Junuk Cha, and Seungryul Baek. Vlm-pl: Advanced pseudo labeling approach for class incremental object detection via vision-language model. In *CVPR*, pages 4170–4181, 2024.
- [25] Rajat Koner, Gagan Jain, Prateek Jain, Volker Tresp, and Sujoy Paul. Lookupvit: Compressing visual information to a limited number of tokens. In *ECCV*, pages 322–337, 2024.
- [26] Ranjay Krishna, Yuke Zhu, Oliver Groth, Justin Johnson, Kenji Hata, Joshua Kravitz, Stephanie Chen, Yannis Kalantidis, Li-Jia Li, David A Shamma, et al. Visual genome: Connecting language and vision using crowdsourced dense image annotations. *International journal of computer vision*, 123:32–73, 2017.
- [27] Qinqian Lei, Bo Wang, and Robby Tan. Ez-hoi: Vlm adaptation via guided prompt learning for zero-shot hoi detection. In *NeurIPS*, pages 55831–55857, 2024.
- [28] Bo Li, Yuanhan Zhang, Dong Guo, Renrui Zhang, Feng Li, Hao Zhang, Kaichen Zhang, Peiyuan Zhang, Yanwei Li, Ziwei Liu, et al. Llava-onevision: Easy visual task transfer. *arXiv preprint arXiv:2408.03326*, 2024.
- [29] Bohao Li, Rui Wang, Guangzhi Wang, Yuying Ge, Yixiao Ge, and Ying Shan. Seed-bench: Benchmarking multimodal llms with generative comprehension. *arXiv preprint arXiv:2307.16125*, 2023.

- [30] Junnan Li, Dongxu Li, Silvio Savarese, and Steven Hoi. Blip-2: Bootstrapping language-image pre-training with frozen image encoders and large language models. In *ICML*, pages 19730–19742, 2023.
- [31] Junnan Li, Dongxu Li, Caiming Xiong, and Steven Hoi. Blip: Bootstrapping language-image pre-training for unified vision-language understanding and generation. In *ICML*, pages 12888–12900, 2022.
- [32] Kevin Y Li, Sachin Goyal, Joao D Semedo, and J Zico Kolter. Inference optimal vlms need only one visual token but larger models. *arXiv preprint arXiv:2411.03312*, 2024.
- [33] Wentong Li, Yuqian Yuan, Jian Liu, Dongqi Tang, Song Wang, Jie Qin, Jianke Zhu, and Lei Zhang. Tokenpacker: Efficient visual projector for multimodal llm. *arXiv preprint arXiv:2407.02392*, 2024.
- [34] Yanwei Li, Chengyao Wang, and Jiaya Jia. Llama-vid: An image is worth 2 tokens in large language models. In *ECCV*, pages 323–340, 2024.
- [35] Yanwei Li, Yuechen Zhang, Chengyao Wang, Zhisheng Zhong, Yixin Chen, Ruihang Chu, Shaoteng Liu, and Jiaya Jia. Mini-gemini: Mining the potential of multi-modality vision language models. *arXiv preprint arXiv:2403.18814*, 2024.
- [36] Yifan Li, Yifan Du, Kun Zhou, Jinpeng Wang, Xin Zhao, and Ji-Rong Wen. Evaluating object hallucination in large vision-language models. In *EMNLP*, 2023.
- [37] Zhang Li, Biao Yang, Qiang Liu, Zhiyin Ma, Shuo Zhang, Jingxu Yang, Yabo Sun, Yuliang Liu, and Xiang Bai. Monkey: Image resolution and text label are important things for large multi-modal models. In *CVPR*, pages 26763–26773, 2024.
- [38] Ji Lin, Hongxu Yin, Wei Ping, Pavlo Molchanov, Mohammad Shoeybi, and Song Han. Vila: On pre-training for visual language models. In *CVPR*, pages 26689–26699, 2024.
- [39] Ziyi Lin, Chris Liu, Renrui Zhang, Peng Gao, Longtian Qiu, Han Xiao, Han Qiu, Chen Lin, Wenqi Shao, Keqin Chen, et al. Sphinx: The joint mixing of weights, tasks, and visual embeddings for multi-modal large language models. *arXiv preprint arXiv:2311.07575*, 2023.
- [40] Haotian Liu, Chunyuan Li, Yuheng Li, and Yong Jae Lee. Improved baselines with visual instruction tuning. In *CVPR*, pages 26296–26306, 2024.
- [41] Haotian Liu, Chunyuan Li, Yuheng Li, Bo Li, Yuanhan Zhang, Sheng Shen, and Yong Jae Lee. Lllavext: Improved reasoning, ocr, and world knowledge, 2024.
- [42] Haotian Liu, Chunyuan Li, Qingyang Wu, and Yong Jae Lee. Visual instruction tuning. In *NeurIPS*, pages 34892–34916, 2023.
- [43] Ting Liu, Liangtao Shi, Richang Hong, Yue Hu, Qianjun Yin, and Linfeng Zhang. Multi-stage vision token dropping: Towards efficient multimodal large language model. *arXiv preprint arXiv:2411.10803*, 2024.
- [44] Yuan Liu, Haodong Duan, Yuanhan Zhang, Bo Li, Songyang Zhang, Wangbo Zhao, Yike Yuan, Jiaqi Wang, Conghui He, Ziwei Liu, et al. Mmbench: Is your multi-modal model an all-around player? In *ECCV*, pages 216–233, 2024.
- [45] Haoyu Lu, Wen Liu, Bo Zhang, Bingxuan Wang, Kai Dong, Bo Liu, Jingxiang Sun, Tongzheng Ren, Zhuoshu Li, Hao Yang, et al. Deepseek-vl: towards real-world vision-language understanding. *arXiv preprint arXiv:2403.05525*, 2024.
- [46] Duc-Tuan Luu, Viet-Tuan Le, and Duc Minh Vo. Questioning, answering, and captioning for zero-shot detailed image caption. In *Proceedings of the Asian Conference on Computer Vision*, pages 242–259, 2024.
- [47] Pingchuan Ma, Lennart Rietdorf, Dmytro Kotovenko, Vincent Tao Hu, and Björn Ommer. Does vlm classification benefit from llm description semantics? In *AAAI*, pages 5973–5981, 2025.

- [48] Ahmed Masry, Do Xuan Long, Jia Qing Tan, Shafiq Joty, and Enamul Hoque. Chartqa: A benchmark for question answering about charts with visual and logical reasoning. *arXiv preprint arXiv:2203.10244*, 2022.
- [49] Minesh Mathew, Viraj Bagal, Rubèn Tito, Dimosthenis Karatzas, Ernest Valveny, and CV Jawahar. Infographicvqa. In *WACV*, pages 1697–1706, 2022.
- [50] Minesh Mathew, Dimosthenis Karatzas, and CV Jawahar. Docvqa: A dataset for vqa on document images. In *WACV*, pages 2200–2209, 2021.
- [51] Anand Mishra, Shashank Shekhar, Ajeet Kumar Singh, and Anirban Chakraborty. Ocr-vqa: Visual question answering by reading text in images. In *ICDAR*, pages 947–952, 2019.
- [52] Artemis Panagopoulou, Le Xue, Ning Yu, Junnan Li, Dongxu Li, Shafiq Joty, Ran Xu, Silvio Savarese, Caiming Xiong, and Juan Carlos Niebles. X-instructblip: A framework for aligning x-modal instruction-aware representations to llms and emergent cross-modal reasoning. *arXiv preprint arXiv:2311.18799*, 2023.
- [53] Alec Radford, Jong Wook Kim, Chris Hallacy, Aditya Ramesh, Gabriel Goh, Sandhini Agarwal, Girish Sastry, Amanda Askell, Pamela Mishkin, Jack Clark, et al. Learning transferable visual models from natural language supervision. In *ICML*, pages 8748–8763, 2021.
- [54] Yuzhang Shang, Mu Cai, Bingxin Xu, Yong Jae Lee, and Yan Yan. Llava-prumerge: Adaptive token reduction for efficient large multimodal models. *arXiv preprint arXiv:2403.15388*, 2024.
- [55] Oleksii Sidorov, Ronghang Hu, Marcus Rohrbach, and Amanpreet Singh. Textcaps: a dataset for image captioning with reading comprehension. In *ECCV*, pages 742–758, 2020.
- [56] Amanpreet Singh, Vivek Natarajan, Meet Shah, Yu Jiang, Xinlei Chen, Dhruv Batra, Devi Parikh, and Marcus Rohrbach. Towards vqa models that can read. In *CVPR*, pages 8317–8326, 2019.
- [57] Dingjie Song, Wenjun Wang, Shunian Chen, Xidong Wang, Michael X Guan, and Benyou Wang. Less is more: A simple yet effective token reduction method for efficient multi-modal llms. In *COLING*, pages 7614–7623, 2025.
- [58] Gemini Team, Petko Georgiev, Ving Ian Lei, Ryan Burnell, Libin Bai, Anmol Gulati, Garrett Tanzer, Damien Vincent, Zhufeng Pan, Shibo Wang, et al. Gemini 1.5: Unlocking multimodal understanding across millions of tokens of context. *arXiv preprint arXiv:2403.05530*, 2024.
- [59] Pavan Kumar Anasosalu Vasu, Fartash Faghri, Chun-Liang Li, Cem Koc, Nate True, Albert Antony, Gokul Santhanam, James Gabriel, Peter Grasch, Oncel Tuzel, et al. Fastvlm: Efficient vision encoding for vision language models. *arXiv preprint arXiv:2412.13303*, 2024.
- [60] Kuo Wang, Lechao Cheng, Weikai Chen, Pingping Zhang, Liang Lin, Fan Zhou, and Guanbin Li. Marvelovd: Marrying object recognition and vision-language models for robust open-vocabulary object detection. In *ECCV*, pages 106–122, 2024.
- [61] Min Wang, Ata Mahjoubfar, and Anupama Joshi. Fashionvqa: A domain-specific visual question answering system. In *CVPR*, pages 3514–3519, 2023.
- [62] Weihang Wang, Qingsong Lv, Wenmeng Yu, Wenyi Hong, Ji Qi, Yan Wang, Junhui Ji, Zhuoyi Yang, Lei Zhao, Song XiXuan, et al. Cogvlm: Visual expert for pretrained language models. *Advances in Neural Information Processing Systems*, 37:121475–121499, 2024.
- [63] Yufei Wang, Zhanyi Sun, Jesse Zhang, Zhou Xian, Erdem Biyik, David Held, and Zackory Erickson. RL-vlm-f: reinforcement learning from vision language foundation model feedback. In *ICML*, pages 51484–51501, 2024.
- [64] Haoran Wei, Lingyu Kong, Jinyue Chen, Liang Zhao, Zheng Ge, Jinrong Yang, Jianjian Sun, Chunrui Han, and Xiangyu Zhang. Vary: Scaling up the vision vocabulary for large vision-language model. In *ECCV*, pages 408–424, 2024.

- [65] Chenyu Yang, Xuan Dong, Xizhou Zhu, Weijie Su, Jiahao Wang, Hao Tian, Zhe Chen, Wenhai Wang, Lewei Lu, and Jifeng Dai. Pvc: Progressive visual token compression for unified image and video processing in large vision-language models. *arXiv preprint arXiv:2412.09613*, 2024.
- [66] Senqiao Yang, Yukang Chen, Zhuotao Tian, Chengyao Wang, Jingyao Li, Bei Yu, and Jiaya Jia. Visionzip: Longer is better but not necessary in vision language models. *arXiv preprint arXiv:2412.04467*, 2024.
- [67] Weihao Yu, Zhengyuan Yang, Linjie Li, Jianfeng Wang, Kevin Lin, Zicheng Liu, Xinchao Wang, and Lijuan Wang. Mm-vet: Evaluating large multimodal models for integrated capabilities. *arXiv preprint arXiv:2308.02490*, 2023.
- [68] Xiang Yue, Yuansheng Ni, Kai Zhang, Tianyu Zheng, Ruoqi Liu, Ge Zhang, Samuel Stevens, Dongfu Jiang, Weiming Ren, Yuxuan Sun, et al. Mmmu: A massive multi-discipline multimodal understanding and reasoning benchmark for expert agi. In *CVPR*, pages 9556–9567, 2024.
- [69] Chenhui Zhang and Sherrie Wang. Good at captioning bad at counting: Benchmarking gpt-4v on earth observation data. In *Proceedings of the IEEE/CVF Conference on Computer Vision and Pattern Recognition*, pages 7839–7849, 2024.
- [70] Qizhe Zhang, Aosong Cheng, Ming Lu, Zhiyong Zhuo, Minqi Wang, Jiajun Cao, Shaobo Guo, Qi She, and Shanghang Zhang. [cls] attention is all you need for training-free visual token pruning: Make vlm inference faster. *arXiv preprint arXiv:2412.01818*, 2024.
- [71] Shaolei Zhang, Qingkai Fang, Zhe Yang, and Yang Feng. Llava-mini: Efficient image and video large multimodal models with one vision token. In *ICLR*, 2025.
- [72] Deyao Zhu, Jun Chen, Xiaoqian Shen, Xiang Li, and Mohamed Elhoseiny. Minigpt-4: Enhancing vision-language understanding with advanced large language models. In *ICLR*, 2024.
- [73] Yuke Zhu, Chi Xie, Shuang Liang, Bo Zheng, and Sheng Guo. Focusllava: A coarse-to-fine approach for efficient and effective visual token compression. *arXiv preprint arXiv:2411.14228*, 2024.